

A Study on Simplifying the Process of a Single Cycle for Multiple Epitaxy and Implantation Method to Fabricate SiC Super Junction

Han-Wei Chen^{1,a*}, Chiao-Yang Cheng^{2,b}, Wei-Liang Lai^{3,c},
Yew-Chung Sermon Wu^{3,d}, Bing-Yue Tsui^{1,e*}

¹Institute of Electronics, National Yang Ming Chiao Tung University, Hsinchu, Taiwan, R.O.C

²The Academy of Innovative Semiconductor and Sustainable Manufacturing, National Cheng Kung University, Tainan, Taiwan, R.O.C

³Department of Materials Science and Engineering, National Yang Ming Chiao Tung University, Hsinchu, Taiwan, R.O.C

^aweich.ee12@nycu.edu.tw, ^b11408019@gs.NCKU.edu.tw, ^ca2289063@gmail.com,
^dsermonwu@nycu.edu.tw, ^ebytsui@nycu.edu.tw

Keywords: Super-junction, Schottky barrier diode, Epitaxial growth, DLTS, SIMS, AFM, Molten KOH.

Abstract. The impact on doping profile, surface roughness and defect production of each process step for a suggested Multiple epitaxy and implantation (MEI) process for Super-junction has been investigated through Secondary Ion Mass Spectrometer (SIMS), Atomic Force Microscope (AFM), Deep Level Transient Spectroscopy (DLTS) and Molten KOH etching. Results show that the suggested process can possibly reduce the cost of the original fabrication and speed up the process.

Introduction

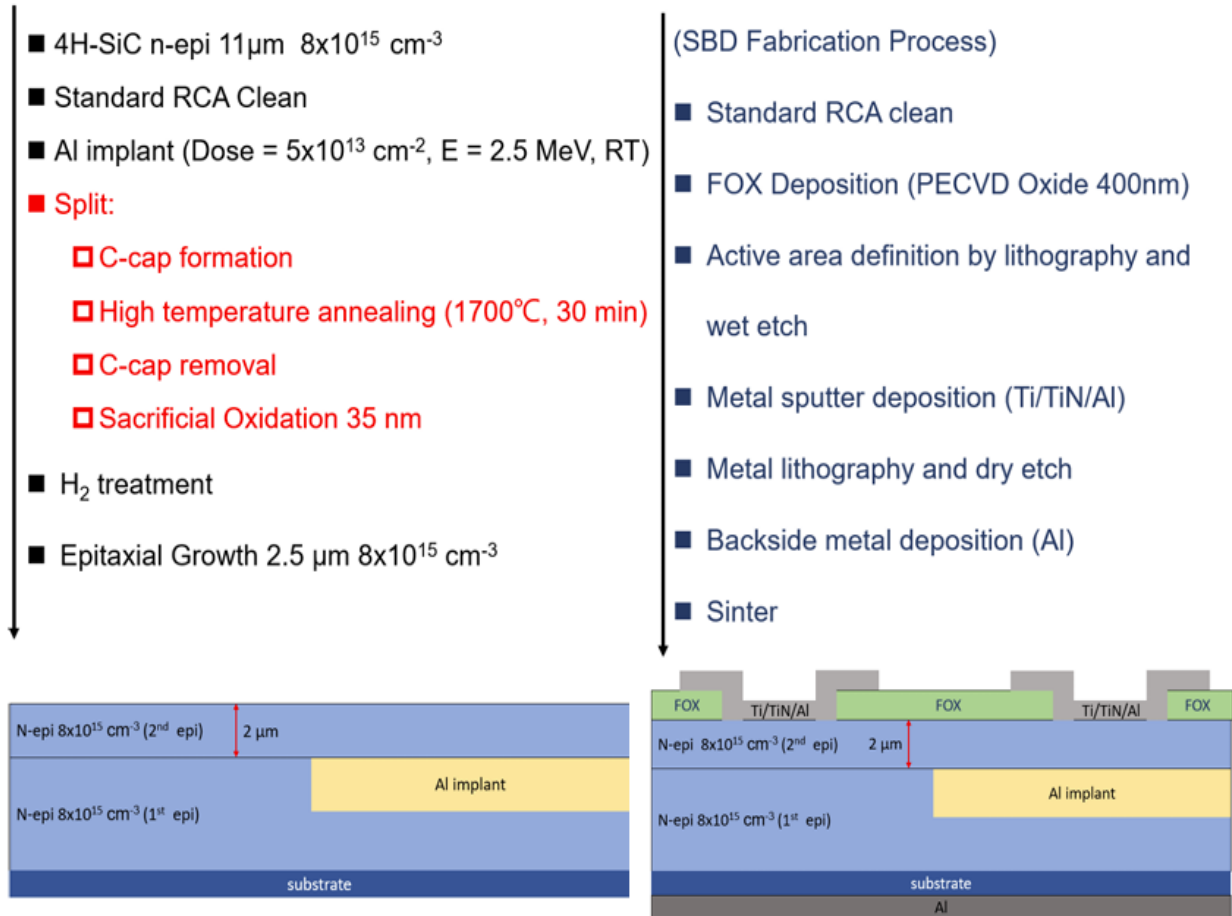
Super-junction (SJ) is known to alleviate the tradeoff between breakdown voltage and specific on-resistance by applying the concept of charge balance [1]. However, the most common fabrication method of SJ structure, Multiple Epitaxy and Implantation (MEI), is time-consuming and costly due to the process complexity [2-3]. On the other hand, hydrogen pretreatment is applied before epitaxial growth, in which the surface is etched and implanted atoms (usually aluminum) may precipitate into the epitaxial chamber. In this work, we examine each step of the MEI process and propose suggestions to simplify the process.

Device Fabrication

Fig.1 shows the main process steps of the experiment, representing one cycle of the MEI process. First, two 4H-SiC n-type epi-wafers with a 11- μm -thick-epi-layer and nitrogen doping concentration of $8.0 \times 10^{15} \text{ cm}^{-3}$ were prepared. Al ion implantation with energy up to 2.5 MeV was carried out with high energy implanter on half of the wafers, with the expectation that no Al atoms would be distributed within the surface layer of 0.3 μm . Next, one wafer was coated with photoresist and baked to form a carbon cap (C-cap) on the SiC surface. Afterwards, the wafer underwent a 1700°C post-implantation annealing (PIA) process for 30 minutes, followed by sacrificial oxidation (to a thickness of 35 nm) after C-cap removal. Surface etching of approximately 0.2 μm by H_2 treatment was performed and the subsequent n-type epi-layer with thickness of 2.5 μm and the same doping concentration was grown on both wafers. Table. 1 lists the sample IDs and split conditions. The quality of the regrown epi-layer was analyzed by Secondary Ion Mass Spectrometer (SIMS), Atomic Force Microscope (AFM), Deep Level Transient Spectroscopy (DLTS) and Molten KOH etching. For DLTS analysis, the samples underwent further process. After a 400-nm-thick PECVD SiO_2 layer was deposited as field oxide, active areas were defined by photo lithography and wet etching processes. Next, Ti/TiN/Al stack were sputtered and patterned, with backside metal deposited in the following step. Finally, the samples were annealed at 500°C for 5 minutes in vacuum and SBD were fabricated.

Table I. Samples ID and process conditions.

Sample	Al implantation	Annealing
I-A	Yes	Yes
NI-A	No	Yes
I-NA	Yes	No
NI-NA	No	No

**Fig. 1.** Process steps, schematic wafer structure and the cross section of Schottky barrier diode (SBD).

Results and Discussion

Fig. 2 shows the depth profile of the I-NA and I-A samples obtained by SIMS. The results are also compared to TCAD simulations. Through the figure, it can be seen that whether or not PIA was performed, the regrown epi-layer did not affect the Al distribution. No Al in the regrown epi-layer was detected, indicating that after neglecting the low-energy ion implantation step, no Al atoms escape into the epitaxial chamber. Fig. 3 shows the surface roughness (R_q) of the four samples measured by AFM. It is expected that implantation without annealing and sacrificial oxidation would increase R_q , which could influence the subsequent epitaxial growth. However, the results show that the R_q values of the four samples are similar, indicating that skipping the annealing and sacrificial processes does not make a significant difference from this perspective.

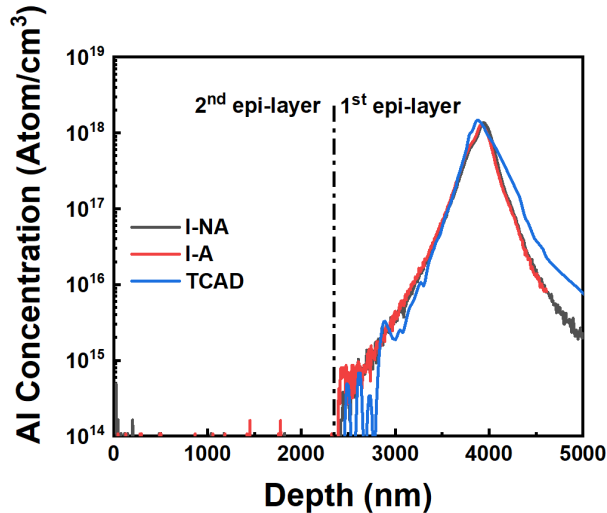


Fig. 2. Secondary Ion Mass Spectrometry (SIMS) depth profiles of Al in the I-NA and I-A samples.

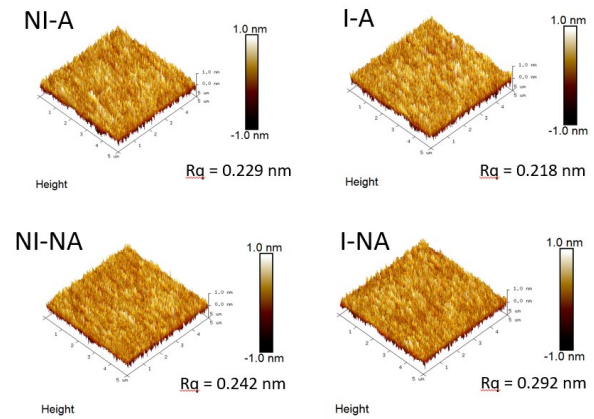


Fig. 3. Atomic Force Microscopy (AFM) surface morphology of the four samples.

The results of DLTS measurements for the samples are shown in Fig. 4. All samples exhibit a similar and weak $Z_{1/2}$ signal, and the defect concentration is approximately $6.85 \times 10^{12} \text{ cm}^{-3}$. The NI-NA sample shows another signal at 400K, which is assumed to be $RD_{1/2}$ with defect density of $3.28 \times 10^{13} \text{ cm}^{-3}$ and may have been generated during epitaxial growth process [4-5]. To verify this assumption, additional samples with epitaxial layers grown using the same equipment were also fabricated into SBDs and examined by DLTS (Fig. 5). It was found that samples exhibited the $RD_{1/2}$ signal did show a defect density of $1.2 \times 10^{12} \sim 3.8 \times 10^{12} \text{ cm}^{-3}$. The following epitaxial might have increased the defect density in the second growth step. On the other hand, the I-NA sample shows a strong signal at 440~460K. Since the samples underwent Al implantation, we assume the signal originates from ON_1 and ON_{2a} [6]. Last, the I-A sample shows an abnormal signal peaked at 500K. Compared with the previous sample, we suppose that annealing and sacrificial oxidation may have converted the defect into new ones due to the high-temperature process, resulting in a signal combining ON_{2a} and ON_{2b} [7-9]. Since the defect concentrations in some samples of I-A and I-NA are similar, if PIA is skipped and the MEI cycle is continued, the overall defect concentration will not be affected, although the defect type may be altered [10].

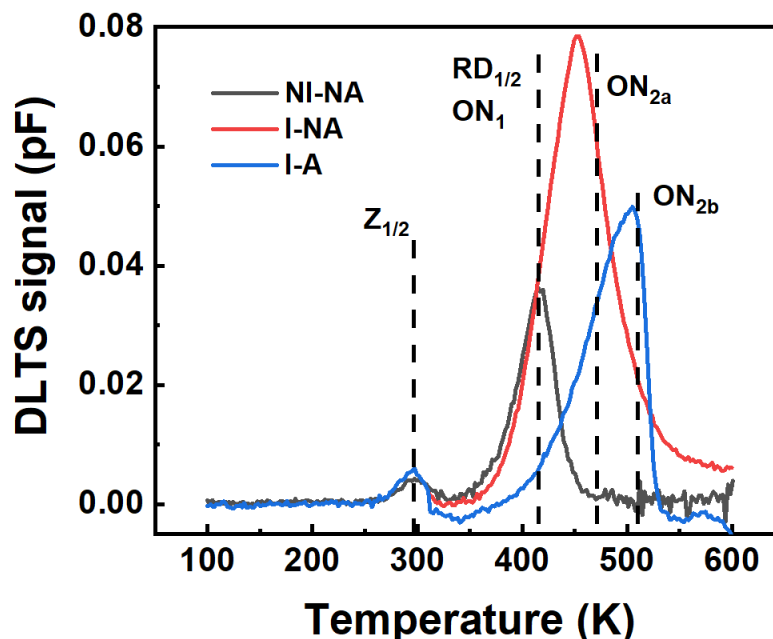


Fig. 4. Deep Level Transient Spectroscopy (DLTS) spectra of the NI-NA, I-NA, and I-A samples.

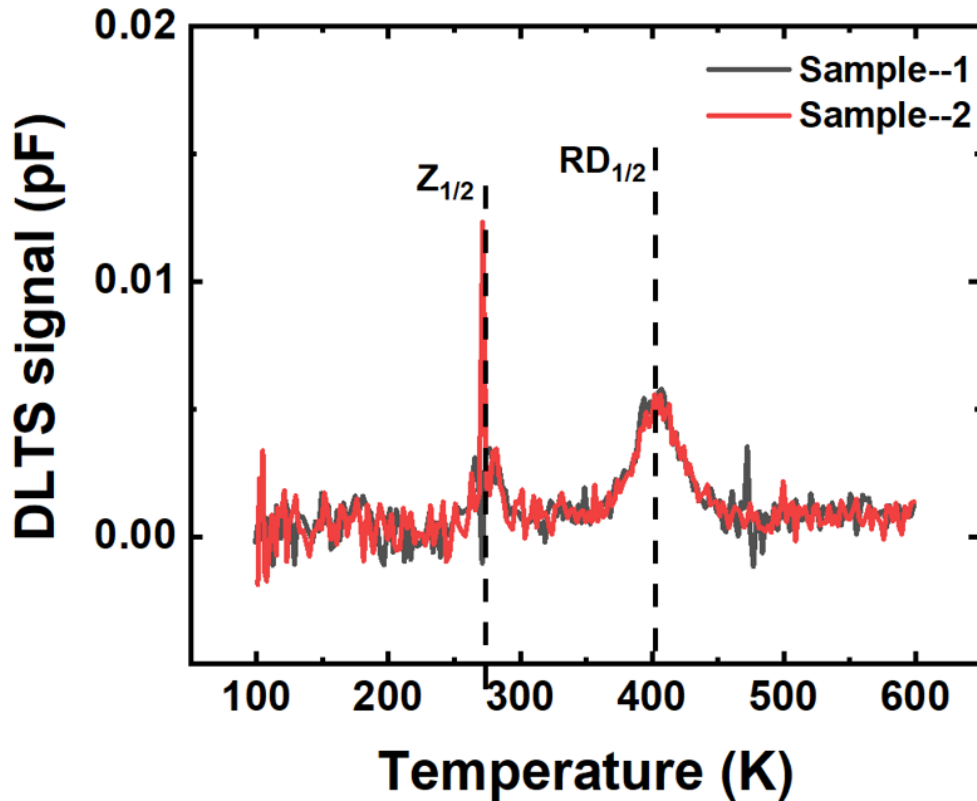


Fig. 5. Deep Level Transient Spectroscopy (DLTS) spectra of other samples with epitaxial growth from the same equipment.

Fig. 6 shows the optical images of the molten KOH-etched surfaces. For I-NA sample, the densities of threading edge dislocations (TEDs) and threading screw dislocations (TSDs) are 1153 cm^{-2} and 192 cm^{-2} , respectively; on the other hand, for I-A sample, the density of TEDs and TSDs are 1077 cm^{-2} and 153 cm^{-2} . These values are comparable to that of typical SiC epitaxial wafers. There is no significant difference in the densities of TEDs between the two samples, indicating that the dislocations are nearly independent of the annealing process in the MEI cycle. However, there is a noticeable difference in the densities of TSDs. The difference can be attributed to the variations in substrate quality. The most influential step affecting the quality of the epitaxial layer is still the regrowth process.

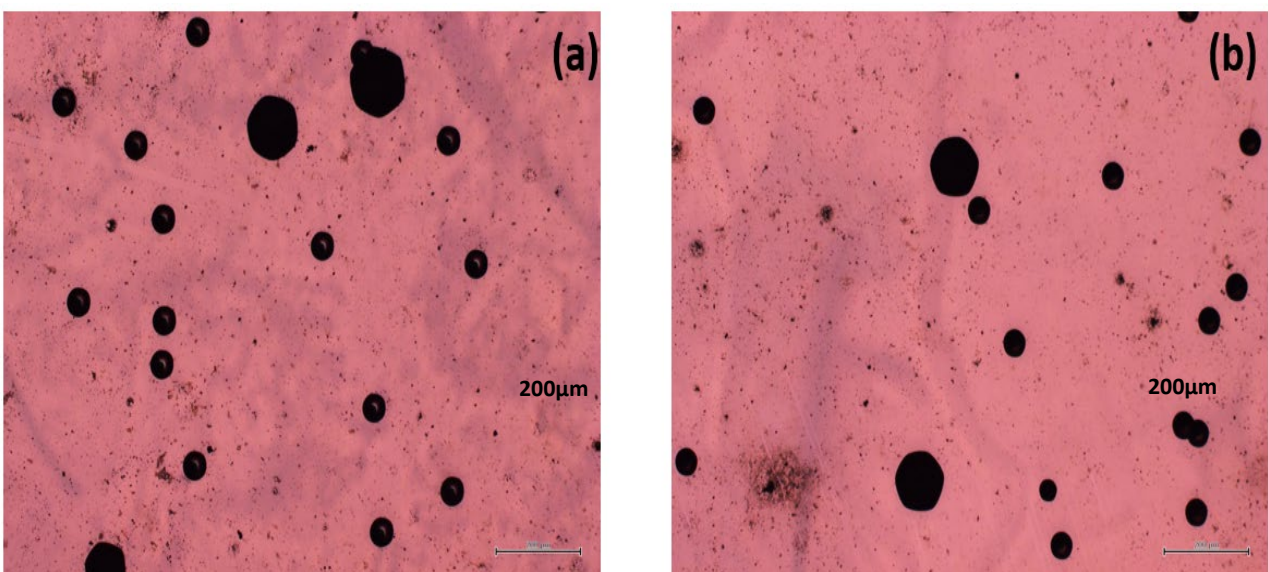


Fig. 6. Image of SiC surface after molten KOH etching of (a) I-NA sample and (b) I-A sample.

Summary

In this work, we examined the impact of each process step of the MEI process on the quality of the subsequent epi-layer. From SIMS analysis, skipping the low-energy implantation prevents Al escape into the epitaxial chamber during growth of the subsequent n-epi layer, thereby avoiding contamination and the following maintenance of the chamber. Moreover, surface roughness and the dislocation density in the subsequent epi-layer are independent of whether PIA is performed. Through DLTS, results indicate that PIA may induce defect transformation, but the slightly increased deep-level defects can be mitigated by the subsequent epitaxial process. The influence of these defects on the electrical characteristics on devices should be further investigated. Nevertheless, if p-pillar ion implantation and subsequent epitaxy can be performed sequentially, the cost and process complexity could be significantly reduced.

Acknowledgement

This work was supported by the National Science and Technology Council, Taiwan, R.O.C. under the contract No. NSTC 113-2218-E-A49-018. Experimental processes were helped by Diodes Inc. and Nano Facility Center of National Yang Ming Chiao Tung University.

References

- [1] T. Fujihira, *Jpn. J. Appl. Phys.* 36 6254, (1997).
- [2] M. Baba et al., 2021 33rd International Symposium on Power Semiconductor Devices and ICs (ISPSD), (2021), 83-86.
- [3] S. Harada et al., 2018 IEEE International Electron Devices Meeting (IEDM), 2018, 8.2.1-8.2.4.
- [4] M. Kato et al., *J. Appl. Phys.*, 100, 5, 053708, (2006).
- [5] L. Ottavianil, *Materials Science Forum*. 457-460, 509–512, (2004).
- [6] P. Kumar et al, *Materials Science in Semiconductor Processing*, 174, 108241, (2024).
- [7] P. Kumar et al., *J. Appl. Phys.*, 135, 18, 185704, (2024).
- [8] M. E Bathen et al, *Materials Science in Semiconductor Processing*, 176, 108316, (2024).
- [9] T. Okuda et al, *Appl. Phys. Express* 8 111301, (2015).
- [10] H F Xiong et al, *J. Semicond.* 45 072502, (2024).